A time reversal algorithm in acoustic media with Dirac measure approximations

Élie Bretin, Carine Lucas, Yannick Privat

▶ **To cite this version:**

Élie Bretin, Carine Lucas, Yannick Privat. A time reversal algorithm in acoustic media with Dirac measure approximations. Inverse Problems, 2018, 34 (4). hal-01529580v2

HAL Id: hal-01529580
https://hal.science/hal-01529580v2

Submitted on 23 Dec 2022

HAL is a multi-disciplinary open access archive for the deposit and dissemination of scientific research documents, whether they are published or not. The documents may come from teaching and research institutions in France or abroad, or from public or private research centers.

L'archive ouverte pluridisciplinaire **HAL**, est destinée au dépôt et à la diffusion de documents scientifiques de niveau recherche, publiés ou non, émanant des établissements d'enseignement et de recherche français ou étrangers, des laboratoires publics ou privés.

A time reversal algorithm in acoustic media with Dirac measure approximations

Élie Bretin* Carine Lucas† Yannick Privat‡

January 28, 2018

Abstract

This article is devoted to the study of a photoacoustic tomography model, where one is led to consider the solution of the acoustic wave equation with a source term writing as a separated variables function in time and space, whose temporal component is in some sense close to the derivative of the Dirac distribution at $t = 0$. This models a continuous wave laser illumination performed during a short interval of time. We introduce an algorithm for reconstructing the space component of the source term from the measure of the solution recorded by sensors during a time T all along the boundary of a connected bounded domain. It is based at the same time on the introduction of an auxiliary equivalent Cauchy problem allowing to derive explicit reconstruction formula and then to use of a deconvolution procedure. Numerical simulations illustrate our approach. Finally, this algorithm is also extended to elasticity wave systems.

1 Introduction and motivations

This article is motivated by some recent applications for medical imaging purposes, namely the so-called *photoacoustic tomography method.* The main idea of the photoacoustic effect is simple: the tissue to be imaged is usually irradiated by a nanosecond-pulsed laser at a given optical wavelength. This energy is converted into heat. Absorption of light by molecules beneath the surface creates a thermally induced pressure jump that propagates as a sound wave, which can be detected. By detecting the pressure waves, we can localize their heterogeneities (i.e., the places where light has been absorbed) and recover important informations about the studied sample [3, 22, 45].

In the sequel, we chose to focus on the photoacoustic method but we mention a very similar hybrid imaging technique called *thermoacoustic tomography* [43, 31, 32, 33] which is based on the generation of acoustic waves by illumination of a sample with a short electromagnetic pulse and for which the method investigated hereafter can be adapted.

A possible model is the following: let us denote by u_0 the pressure generated by the thermal expansion of tissues. Let Ω be a smooth bounded domain in $\mathbb{R}^d$ with $d = 2, 3$. One considers the standard acoustic wave equation

$$\begin{cases} \partial_{tt} u_0(t,x) - \Delta u_0(t,x) = \frac{d\delta_0}{dt} H(x), & (t,x) \in \mathbb{R} \times \mathbb{R}^d, \\ u_0(t,\cdot) = \partial_t u_0(t,\cdot) = 0, & t < 0, \end{cases} \tag{1.1}$$

where δ_0 stands for the Dirac measure with respect to the time variable t at $t = 0$ and $H \in L^2(\mathbb{R}^d, \mathbb{R})$ denotes the absorbed optical energy, in other words the initial source term resulting from the expansion of tissues [28, 41].

Notice that the presence of the derivative of the Dirac term at $t = 0$ denoted $\frac{d\delta_0}{dt}$, models a short pulsed illumination at $t = 0$. From a practical point of view, such a model appears irrelevant in some experimental situations where one uses multiples ultrashort laser pulses with a minimal pulse energy to

*CNRS UMR 5208, INSA de Lyon, Institut Camille Jordan, Université de Lyon, 20, avenue Albert Einstein, 69621 Villeurbanne Cedex, France (elie.bretin@insa-lyon.fr)

†Université d'Orléans, Labo. MAPMO, CNRS, UMR 6628, Fédération Denis Poisson, FR 2964, Bat. Math., BP 6759, 45067 Orléans cedex 2, France (carine.lucas@univ-orleans.fr).

‡CNRS, Sorbonne Universités, UPMC Univ Paris 06, UMR 7598, Laboratoire Jacques-Louis Lions, F-75005, Paris, France (yannick.privat@upmc.fr).

avoid laser damages, but with sufficiently high-energy deposition to ensure a satisfactory signal-to-noise ratio [36, 44]. In such a case, the right-hand-side in the p.d.e. model (1.1) has to be modified and leads to consider rather the equation

$$\begin{cases} \partial_{tt} u_\varepsilon(t,x) - \Delta u_\varepsilon(t,x) = \dfrac{df_\varepsilon}{dt}(t) H(x), & (t,x) \in \mathbb{R}^d \times \mathbb{R}, \\ u_\varepsilon(t,\cdot) = \partial_t u_\varepsilon(t,\cdot) = 0, & t < -\varepsilon T_f, \end{cases} \tag{1.2}$$

where f_ε is defined for a small parameter $\varepsilon > 0$ by

$$f_\varepsilon(t) = \frac{1}{\varepsilon} f\left(\frac{t}{\varepsilon}\right), \tag{1.3}$$

and $f \in C^1(\mathbb{R})$ is a known excitation function whose support is included in $[-T_f, T_f]$ with $T_f > 0$. It is well-known that, with such a choice, the sequence of functions $(df_\varepsilon/dt)_{\varepsilon>0}$ converges to $d\delta_0/dt$ in the sense of distributions.

Furthermore, the source term $H(\cdot) \in L^2(\mathbb{R}^d)$ is assumed to have a support compactly included in a connected bounded domain Ω with $\mathrm{dist}(\mathrm{supp}(H), \partial\Omega) > 0$.

Note that, in this work, we are not concerned with the so-called "quantitative part" of the photoacoustic technique (see e.g. [1, 11, 12, 17]) but only with the issue of recovering the source term H.

Let us introduce the function g_ε, standing for the information recorded by sensors on the boundary of Ω during a time T, defined by

$$g_\varepsilon(t,y) = u_\varepsilon(t,y) \qquad \text{for all } t \in [0,T] \text{ and } y \in \partial\Omega, \tag{1.4}$$

where T is supposed to be sufficiently large to satisfy $u_\varepsilon(t,\cdot) \simeq 0$ and $\partial_t u_\varepsilon(t,\cdot) \simeq 0$ in Ω, for every $t > T$ whenever $d = 2$ or $u_\varepsilon(t,\cdot) = \partial_t u_\varepsilon(t,\cdot) = 0$, for every $t > T$ whenever $d = 3$. Notice that the existence of such a time follows from the so-called Huyghens principle (see e.g. [24, Section 2.4]). The (imprecise) notation "$\simeq$" used above (for the sake of simplicity) will be commented at the beginning of Section 4 after.

The motivation of this work is to provide an algorithm allowing to reconstruct an approximation of the source term $H(\cdot)$ from the knowledge of the given data g_ε on $\partial\Omega \times [0,T]$.
In many applications, the pulse is assumed to be a good approximation of the Dirac distribution derivative at $t = 0$, so that the model (1.1) appears relevant. In this setting, one can prove that the acoustic wave solution also solves the Cauchy problem

$$\begin{cases} \partial_{tt} u_0(t,x) - \Delta u_0(t,x) = 0, & (t,x) \in \mathbb{R}_+ \times \mathbb{R}^d, \\ u_0(0,x) = H(x), \quad \partial_t u_0(0,x) = 0, & x \in \mathbb{R}^d. \end{cases} \tag{1.5}$$

In this framework, the linear inverse problem which consists in reconstructing H from given data g_0 as defined by (1.4), can then be easily solved by using for instance the time reversal algorithm [13, 5, 26, 30] or inversion formula such as the spherical Radon transform [7, 25, 35, 38, 39], or variational techniques [15]. In particular, an error estimate is derived in [29] which shows the stability of the time reversal imaging approach.

However, in many applications and typically when dealing with the photoacoustic tomography technique with a continuous pulse performed during a short time, the parameter ε is not small enough to replace the right-hand side by the term $d\delta_0/dt$, so that System (1.2) has to be considered instead of System (1.1). In such a case, the previous strategy cannot be used as well.

For instance, in the recent paper [18], the authors propose to correct the data g_ε by using a deconvolution algorithm associated to the kernel f_ε and then to apply the time reversal imaging on the corrected data. A difficulty of such an approach is that a deconvolution algorithm rests upon the regularity of the data whereas g_ε is not smooth at $\varepsilon = 0$ even if the source H is smooth (see Figure 2).

In this article, we introduce an alternative approach which consists to apply the classical time reversal imaging on the uncorrected data g_ε to obtain an approximation H_ε of the source H. We then explain how we can correct the effect of ε on H_ε by using a deconvolution algorithm where the kernel

can be built explicitly and depends only on ε and f. One advantage of this approach is that a deconvolution algorithm can be easily used on H_ε as soon as the source H satisfies good smoothness properties.

The rest of the paper is organized as follows. The main results of this article including the complete description of the reconstruction algorithm are stated in Section 2.1. In section 2.2, we gather some tools including useful identities about the Green function Γ associated to the wave equation. The proofs of the main results are postponed to Section 3. Finally, we provide in Section 4 some numerical illustrations highlighting the potential of our approach.

2 Description of the algorithm

2.1 Strategy and main results

The key point of the algorithm we will introduce rests upon the introduction of an *equivalent Cauchy problem* to System (1.2) of the form

$$\begin{cases} \partial_{tt} v_\varepsilon(t,x) - \Delta v_\varepsilon(t,x) = 0, & (t,x) \in \mathbb{R}^d \times \mathbb{R}_+, \\ v_\varepsilon(0,x) = H_\varepsilon(x), \quad \partial_t v_\varepsilon(0,x) = G_\varepsilon(x), & x \in \mathbb{R}^d, \end{cases} \tag{2.1}$$

the wording *equivalent* meaning that, if u_ε denotes the solution of (1.2) and g_ε denotes the data measured on the boundary:

$$g_\varepsilon(t,y) = u_\varepsilon(t,y) = v_\varepsilon(t,y), \qquad \text{for all } t > 0 \text{ and } y \in \partial\Omega.$$

In other words, the notion of equivalence of problems is related to the choice of the domain Ω and it means that the data recorded on the boundary $\partial\Omega$ by using (2.1) and (1.2) are the same.

In the sequel, we will assume that the support of the source H in (1.2) is included in a compact subset K of Ω. Using that the support of f_ε is contained in $[-\varepsilon T_f, \varepsilon T_f]$, we will show the existence of an equivalent Cauchy problem provided that

$$4\varepsilon T_f \leq d_K, \quad \text{with} \quad \operatorname{dist}(K, \partial\Omega) = d_K, \tag{2.2}$$

that is the parameter ε is sufficiently small such that the boundary is quite far from the source compared to the length of the support of f_ε.

Under such assumptions, we will build two operators $\mathcal{L}_1$ and $\mathcal{L}_2$ such that

$$H_\varepsilon = \mathcal{L}_1[f_\varepsilon, H], \quad G_\varepsilon = \mathcal{L}_2[f_\varepsilon, H],$$

whose expressions will be fully explicit.

Then, the reconstruction procedure of the source term H from the data g_ε will be performed into two steps:

Step 1. Knowing the pulse f_ε (approximating the Dirac measure $\delta_{t=0}$), determination of the source term H_ε in (2.1) from the knowledge of g_ε by using an approach either based on a standard time reversal algorithm or on a spherical radon transform. Notice that there is an abundant literature about the aforementioned methods. One can refer for instance to [5, 7] for more explanations about them.

Step 2. Reconstruction of the source H from the knowledge of H_ε. In this view, we use a deconvolution algorithm combined with the knowledge of the operators $\mathcal{L}_i$, $i = 1, 2$ such that

$$H_\varepsilon = \mathcal{L}_1[f_\varepsilon, H], \quad G_\varepsilon = \mathcal{L}_2[f_\varepsilon, H].$$

In what follows, we will focus on Step 2, by providing an explicit reconstruction formula. For that purpose, we will use an explicit representation of the solution of (1.2) combined with the so-called time reversal principle to exploit the data measured by the sensors (modeled by the function g_ε, see (1.4)).

The whole procedure is illustrated on Figure 1 and is described with more details at the end of this section.

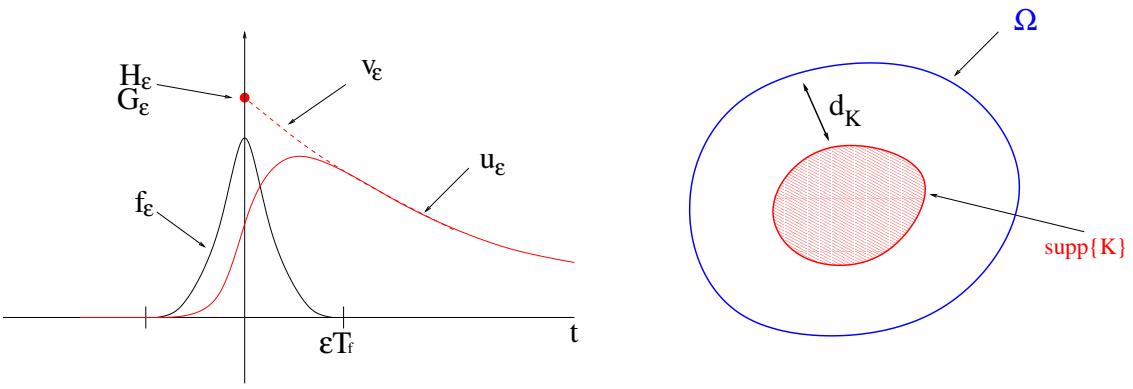

Figure 1: Principle of the time reversal approach

Notations. The following notations will be used throughout the paper.

- $|\cdot|$: euclidean norm in $\mathbb{R}^d$;
- $\Box := \partial_{tt} - \Delta$ (the d'Alembert operator);
- If $f : \mathbb{R} \to \mathbb{R}$ is a function, the notation f_o (resp. f_e) stand for the odd (resp. even) part of f;
- For $x_0 \in \mathbb{R}^d$ (resp. $t_0 \in \mathbb{R}$), $\delta_{\{x=x_0\}}$ or simply δ_{x_0} when no confusion is possible (resp. $\delta_{\{t=t_0\}}$) denotes the Dirac distribution at $x = x_0$ (resp. at $t = t_0$).
- The operator $\mathcal{F}_t$ (resp. $\mathcal{F}_x$) stands for the Fourier transform in time (resp. in space), in other words for every $H \in L^1(\mathbb{R}^d)$ and $f \in L^1(\mathbb{R})$, one has

$$\mathcal{F}_t[f] : \mathbb{R} \ni \omega \mapsto \int_{\mathbb{R}} f(t)e^{-it\omega}\, dt \quad \text{and} \quad \mathcal{F}_x[H] : \mathbb{R}^d \ni \xi \mapsto \int_{\mathbb{R}^d} H(x)e^{-ix\cdot\xi}\, dx.$$

- For S and T two distributions having a compact support, the convolution product $S * T$ is defined by (with obvious notations)

$$\forall \varphi \in \mathcal{D}(\mathbb{R}^d), \quad \langle S * T, \varphi\rangle = \langle S_x \langle T_y, \varphi(x+y)\rangle\rangle.$$

- If X denotes a subset of $\mathbb{R}^d$, χ_X stands for the characteristic function of X, that is the function equal to 1 on X and 0 elsewhere.

Warning about notations and abuses of notation. In the sequel, to make the distinction between space and time convolutions easier, we will denote by $\int_{\mathbb{R}} f(s)g(t-s)\, ds$ the convolution product in time between f and g, even if f and g are two (supported on a half line or on a compact set) distributions.

Main result. The main result of this article concerns the rewriting of the source terms H_ε and G_ε as convolution products of H and a kernel, namely

$$H_\varepsilon = H * K_{1,f_\varepsilon} \quad \text{and} \quad G_\varepsilon = H * K_{2,f_\varepsilon}$$

where the expression of the two kernels K_{1,f_ε} and K_{2,f_ε} is fully explicit (see Theorem 2.1 below).

Let us introduce the Green function Γ of the wave equation, namely the solution in a distributional sense of the following Cauchy problem

$$\begin{cases} \partial_{tt}\Gamma(t,x) - \Delta\Gamma(t,x) = 0 & (t,x) \in \mathbb{R}^d \times \mathbb{R}_+, \\ \Gamma(0,\cdot) = 0, \quad \partial_t\Gamma(0,\cdot) = \delta_{\{x=0\}}. \end{cases} \tag{2.3}$$

Theorem 2.1. *Let $T_f > 0$, $\varepsilon > 0$, Ω be a connected bounded open set of $\mathbb{R}^d$ and K be a compact set such that $K \subset \Omega$. Under the condition (2.2) on ε and K, for all $H \in L^2(\mathbb{R}^d)$ such that $\mathrm{supp}(H) \subset K$, there exists a Cauchy problem of the form (2.1) equivalent to (1.2) in the sense made precise above. Moreover, H_ε and G_ε are given by*

$$H_\varepsilon = \mathcal{L}_1[f_\varepsilon, H] = H * K_{1,f_\varepsilon}, \qquad \text{and} \qquad G_\varepsilon = \mathcal{L}_2[f_\varepsilon, H] = H * K_{2,f_\varepsilon},$$

where

$$K_{1,f_\varepsilon}(\cdot) = \int_{\mathbb{R}} \partial_t \Gamma(s,\cdot) f_\varepsilon(s)\, ds \quad \text{and} \quad K_{2,f_\varepsilon}(\cdot) = \int_{\mathbb{R}} \partial_{tt} \Gamma(s,\cdot) f_\varepsilon(s)\, ds,$$

these last expressions being understood as duality pairing of the space of Radon measures on $\mathbb{R}$ with $C^0(\mathbb{R})$.

Furthermore if $(f_\varepsilon)_{\varepsilon>0}$ converges to $\delta_{\{t=0\}}$ in the sense of distributions, then K_{1,f_ε} (resp. K_{2,f_ε}) converges to $\delta_{\{x=0\}}$ (resp. 0) in the sense of distributions.

The proof of this theorem is postponed to Section 3.1.

We complete the theorem above by providing an explicit expression of the kernels K_{1,f_ε} and K_{2,f_ε}, which appears workable from a numerical point of view when performing all computations in the Fourier space.

Proposition 2.2. *Let $f \in L^2(\mathbb{R})$ be defined from its Fourier transform $\hat{f}$ by*

$$\hat{f}(\omega) = \sum_{n=0}^{+\infty} \alpha_n \omega^n,$$

where $(\alpha_n)_{n\in\mathbb{N}}$ is a sequence of real numbers.

Let us assume that:

(H) *the Fourier transform $\hat{f}$ is real-analytic in $\mathbb{R}$.*

Then, one has

$$K_{1,f_\varepsilon}(x) = \mathcal{F}_x^{-1}\left[\hat{f}_e(|\xi|\varepsilon)\right] \qquad \text{and} \qquad K_{2,f_\varepsilon}(x) = i\mathcal{F}_x^{-1}\left[|\xi|\hat{f}_o(|\xi|\varepsilon)\right],$$

where f_e and f_o denote respectively the even and odd parts of f.

In particular, if $f : \mathbb{R} \ni t \mapsto \frac{1}{(4\pi)^{d/2}} \exp(-\frac{t^2}{4})$, then

$$K_{1,f_\varepsilon}(x) = \frac{1}{(4\varepsilon\pi)^{d/2}} \exp\left(-\frac{|x|^2}{4\varepsilon^2}\right) = \mathcal{F}_x^{-1}\left[\exp(-|\xi|^2\varepsilon^2)\right](x) \qquad \text{and} \qquad K_{2,f_\varepsilon}(x) = 0.$$

Remark 2.3 (Comments on the assumption (H).)**.** *Writing this proposition, we had not in mind to look for the sharpest assumptions ensuring the validity of this result, but rather to cover some standard cases, such as the gaussian one. Notice that these equalities also holds whenever f denotes the characteristic function of an interval. It is notable that the analyticity of Fourier transforms is closely related to the speed of decreasing of the function f. One can refer to [37] or to [42] for issues related to the Paley-Wiener theorem. Finally, it is notable that, if f is assumed to have an exponential decay, namely that $f(x)\exp(\alpha|x|) \in L^1(\mathbb{R})$ for some $\alpha > 0$, then its Fourier transform extends to an analytic function on a strip of the complex plane and is therefore analytic on $\mathbb{R}$. This covers in particular the case of pulses f having compact support in $\mathbb{R}$.*

From these results, we derive an algorithm that will be introduced and commented in Section 4.

2.2 Some reminders about Green functions for the wave equation

It is notable that the Green function Γ defined by (2.3) coincides with the solution in a distributional sense of the Cauchy problem

$$\begin{cases} \partial_{tt}\Gamma(t,x) - \Delta\Gamma(t,x) = \delta_{\{t=0\}}\delta_{\{x=0\}} & (t,x) \in \mathbb{R}_+ \times \mathbb{R}^d, \\ \Gamma(t,\cdot) = \partial_t\Gamma(t,\cdot) = 0, & t < 0. \end{cases} \tag{2.4}$$

Lemma 2.4. *Let $T > 0$ and $F \in L^2(\mathbb{R}, L^2(\mathbb{R}^d))$ be such that $F(t,\cdot) = 0$ whenever $t < -T$. Then, the distributional solution U of $\Box U = F$ such that $U = 0$ whenever $t < -T$ is*

$$U(t,\cdot) = \int_{\mathbb{R}} F(s,\cdot) * \Gamma(t-s,\cdot)\, ds \quad \forall t \geq -T,$$

where the convolution product $*$ operates between functions of the space variable x.

Notice that the temporal Green function $\Gamma(t,\cdot)$ can also be obtained as the inverse Fourier transform of Γ_ω

$$\Gamma(t,\cdot) = \mathcal{F}_t^{-1}[\Gamma_\omega(\cdot)](t),$$

where Γ_ω denotes the outgoing fundamental solution to the Helmholtz operator $-(\Delta + \omega^2)$ in $\mathbb{R}^d$, that is the distributional solution of the equation

$$(\Delta + \omega^2)\Gamma_\omega(x) = -\delta_{\{x=0\}} \qquad x \in \mathbb{R}^d$$

subject to the outgoing Sommerfeld radiation equation

$$\lim_{|x|\to\infty} |x|^{\frac{d-1}{2}} \left(\frac{\partial}{\partial|x|} - ik\right) \Gamma_\omega(x) = 0.$$

Lemma 2.5. *For H and G in $L^2(\mathbb{R}^d)$ with compact support, if u solves the following wave equation in a distributional sense*

$$\begin{cases} \partial_{tt}u(t,x) - \Delta u(t,x) = H(x)\frac{d\delta_{\{t=0\}}}{dt} + G(x)\delta_{\{t=0\}} & (t,x) \in \mathbb{R}\times\mathbb{R}^d, \\ u(t,\cdot) = \partial_t u(t,\cdot) = 0 & t < 0, \end{cases} \tag{2.5}$$

then, the restriction of u to positive times (still denoted by u with a slight abuse of notation) solves the p.d.e.

$$\begin{cases} \partial_{tt}u(t,x) - \Delta u(t,x) = 0 & (t,x) \in \mathbb{R}_+\times\mathbb{R}^d, \\ u(0,\cdot) = H(\cdot), \quad \partial_t u(0,\cdot) = G(\cdot) \end{cases} \tag{2.6}$$

and we have

$$\forall t \geq 0, \quad \begin{cases} u(t,\cdot) &= H * \partial_t\Gamma(t,\cdot) + G * \Gamma(t,\cdot) \\ \partial_t u(t,\cdot) &= H * \partial_{tt}\Gamma(t,\cdot) + G * \partial_t\Gamma(t,\cdot), \end{cases} \tag{2.7}$$

where the convolution product $*$ operates between functions of the space variable x.

Remark 2.6. *Notice that the regularity assumptions on H and G guarantee that they belong to $L^1_{loc}(\mathbb{R}^d)$ and therefore, define distributions. Moreover, the convolution products in (2.7) make sense since H and G have compact support.*

Proof. Let Y denote the Heaviside step function. Let us denote temporarily by $\tilde{u}$ the restriction of u to positive times, in other words $u = Y\tilde{u}$. Then, we get that $\tilde{u}$ solves System (2.6) by plugging its expression into (2.5).

Let us show the first equality of (2.7), the second one being proved by similar arguments. Introduce the distribution $z = H * \partial_t\Gamma(t,\cdot)$. There holds

$$\begin{aligned} \Box z(t,\cdot) &= \partial_{tt}(H * \partial_t\Gamma(t,\cdot)) - \Delta(H * \partial_t\Gamma(t,\cdot)) \\ &= H * \partial_{tt}\partial_t\Gamma(t,\cdot) - H * \Delta\partial_t\Gamma(t,\cdot) = H * \partial_t\Box\Gamma(t,\cdot) \\ &= \frac{d\delta_{\{t=0\}}}{dt} H * \delta_{\{x=0\}} = \frac{d\delta_{\{t=0\}}}{dt} H. \end{aligned}$$

Therefore, z solves the main equation of (2.6) and one checks that $z(0,\cdot) = H(\cdot)$ and $\partial_t z(0,\cdot) = 0$. Mimicking this reasoning with the distribution $\tilde{z} = G * \Gamma(t,\cdot)$ yields that $\tilde{z}$ solves the main equation of (2.6) and one checks that $\tilde{z}(0,\cdot) = 0$ and $\partial_t\tilde{z}(0,\cdot) = G(\cdot)$. By uniqueness of the solution of (2.6), we easily infer that $u = z + \tilde{z}$. □

We then deduce the following rewriting of the Green function Γ and its time derivative.

Proposition 2.7. *For all $t \in [0,s]$, we have*

$$\begin{cases} \partial_t\Gamma(t,\cdot) &= \partial_t\Gamma(s-t,\cdot) * \partial_t\Gamma(s,\cdot) - \partial_{tt}\Gamma(t,\cdot) * \Gamma(s-t,\cdot) \\ \Gamma(t,\cdot) &= \Gamma(t,\cdot) * \partial_t\Gamma(s-t,\cdot) - \partial_t\Gamma(t,\cdot) * \Gamma(s-t,\cdot) \end{cases} \quad \text{in } \mathcal{D}'(\mathbb{R}^d).$$

In particular, considering $t = 0$, we obtain the identity:

$$\forall s > 0, \qquad \delta_{\{x=0\}} = \partial_t\Gamma(s,\cdot) * \partial_t\Gamma(s,\cdot) - \partial_{tt}\Gamma(s,\cdot) * \Gamma(s,\cdot) \tag{2.8}$$

Proof. For all $s > 0$ and $t \in [0,s]$, the time reversal principle shows that, if u is the solution of (2.5), the function v defined by $v(s,\cdot) = u(s-t,\cdot)$ solves the wave equation

$$\begin{cases} \partial_{tt}v(t,x) - \Delta v(t,x) = 0 & (t,x) \in [0,s] \times \mathbb{R}^d, \\ v(0,\cdot) = u(s,\cdot), \quad \partial_t v(0,\cdot) = \partial_t u(s,\cdot). \end{cases} \tag{2.9}$$

Let $t \in [0,s]$. According to Lemma 2.5,

$$\begin{aligned} u(t,\cdot) &= v(s-t,\cdot) \\ &= u(s,\cdot) * \partial_t\Gamma(s-t,\cdot) - \partial_t u(s,\cdot) * \Gamma(s-t,\cdot) \\ &= (H * \partial_t\Gamma(s,\cdot) + G * \Gamma(s,\cdot)) * \partial_t\Gamma(s-t,\cdot) - (H * \partial_{tt}\Gamma(s,\cdot) + G * \partial_t\Gamma(s,\cdot)) * \Gamma(s-t,\cdot) \\ &= H * (\partial_t\Gamma(s-t,\cdot) * \partial_t\Gamma(s,\cdot) - \partial_{tt}\Gamma(s,\cdot) * \Gamma(s-t,\cdot)) \\ &\quad + G * (\Gamma(s,\cdot) * \partial_t\Gamma(s-t,\cdot) - \partial_t\Gamma(s,\cdot) * \Gamma(s-t,\cdot)). \end{aligned}$$

Moreover, since

$$u(t,\cdot) = H * \partial_t\Gamma(t,\cdot) + G * \Gamma(t,\cdot)$$

and since these relations hold for any arbitray functions H and G, we get the expected result. □

In the sequel, it will be useful to use the following identities about Green's functions.

Proposition 2.8. *For all $p \in \mathbb{N}$,*

$$\int_{\mathbb{R}} (-1)^p \omega^{2p} i\omega\Gamma_\omega(\cdot)\, d\omega = \Delta^p(\delta_{\{x=0\}}) \quad \text{and} \quad \int_{\mathbb{R}} (-1)^p \omega^{2p}\Gamma_\omega(\cdot)\, d\omega = 0.$$

Proof. According to Eq. (2.3), one has

$$\Gamma(0,.) = 0, \qquad \text{and} \qquad \partial_t\Gamma(0,.) = \delta_{\{x=0\}},$$

and by induction, we infer that

$$\forall n \in \mathbb{N}, \quad \frac{\partial^n\Gamma}{\partial t^n}(0,\cdot) = \begin{cases} \Delta^{(n-1)/2}(\delta_{\{x=0\}}), & \text{if } n \text{ is odd} \\ 0 & \text{if } n \text{ is even,} \end{cases}$$

where the distribution $\Delta^p(\delta_{\{x=0\}})$ is defined for $p \in \mathbb{N}^*$ by

$$\langle \Delta^p(\delta_{\{x=0\}}), \varphi \rangle = \Delta^p\varphi|_{\{x=0\}}, \quad \forall \varphi \in \mathcal{D}(\mathbb{R}^d).$$

The expected conclusion is obtained by reading these last identities in the Fourier space. □

3 Proofs of the main results

3.1 Proof of Theorem 2.1

Equivalent Cauchy problem. Let us first introduce the solution w_ε of the acoustic wave equation

$$\begin{cases} \partial_{tt}w_\varepsilon(t,x) - \Delta w_\varepsilon(t,x) = 0, & (t,x) \in [0,\varepsilon T_f] \times \mathbb{R}^d, \\ w_\varepsilon(0,x) = u_\varepsilon(\varepsilon T_f, x), \quad \partial_t w_\varepsilon(0,x) = -\partial_t u_\varepsilon(\varepsilon T_f, x), & x \in \mathbb{R}^d. \end{cases} \tag{3.1}$$

and consider H_ε and G_ε defined by

$$H_\varepsilon(\cdot) = w_\varepsilon(\varepsilon T_f, \cdot), \quad \text{and} \quad G_\varepsilon(\cdot) = -\partial_t w_\varepsilon(\varepsilon T_f, \cdot).$$

Let us show that such choices of H_ε and G_ε as initial data for System (2.1) yield an equivalent problem to (1.2). First, according to the time reversal principle (illustrated on Figure 1), we have

$$u_\varepsilon(x,t) = v_\varepsilon(x,t), \forall x \in \mathbb{R}^d,$$

for every $t \geq \varepsilon T_f$.

Since $2\varepsilon T_f < d_K$, we infer that

$$u_\varepsilon(t,y) = 0, \quad \forall (t,y) \in [0, \varepsilon T_f] \times \partial\Omega.$$

by using the finite time propagation property of the wave equation.

Moreover, using now that $4\varepsilon T_f < d_K$ and by (still) using the finite time propagation property of the wave equation, we get that

$$\text{dist}(\text{supp}(u_\varepsilon(\varepsilon T_f, \cdot), \partial\Omega) \geq d_K - 2\varepsilon T_f, \quad \text{dist}(\text{supp}(\partial_t u_\varepsilon(\varepsilon T_f, \cdot), \partial\Omega) \geq d_K - 2\varepsilon T_f,$$

and

$$\text{dist}(\text{supp}(H_\varepsilon), \partial\Omega) \geq d_K - 3\varepsilon T_f, \quad \text{dist}(\text{supp}(G_\varepsilon), \partial\Omega) \geq d_K - 3\varepsilon T_f.$$

This yields that

$$\text{dist}(\text{supp}(v_\varepsilon), \partial\Omega) \geq d_K - 3\varepsilon T_f - t,$$

for all $t \in [0, \varepsilon T_f]$ which means that

$$v_\varepsilon(t,y) = 0, \quad \forall (t,y) \in [0, \varepsilon T_f] \times \partial\Omega.$$

Finally, we proved that

$$u_\varepsilon(t,y) = v_\varepsilon(t,y), \quad \forall (t,y) \in \mathbb{R}_+ \times \partial\Omega.$$

Expression of $\mathcal{L}_1[f_\varepsilon, H]$ and $\mathcal{L}_2[f_\varepsilon, H]$. Notice that the operator $\mathcal{L}_1$ can be also defined as

$$\mathcal{L}_1[f_\varepsilon, H] = H_\varepsilon = w_\varepsilon(\varepsilon T_f, \cdot).$$

According to Lemma 2.5,

$$\mathcal{L}_1[f_\varepsilon, H] = u_\varepsilon(\varepsilon T_f, x) * \partial_t \Gamma(\varepsilon T_f, \cdot) - \partial_t u_\varepsilon(\varepsilon T_f, \cdot) * \Gamma(\varepsilon T_f, \cdot).$$

Moreover, by using Lemma 2.4, since u_ε solves the p.d.e. (1.2) (notice that in particular $\Box u_\varepsilon = 0$ as $t \geq \varepsilon T_f$), one has for all $t \geq \varepsilon T_f$,

$$u_\varepsilon(t,x) = H * \left(\int_{\mathbb{R}} f_\varepsilon(s) \partial_t \Gamma(t-s, \cdot)\, ds \right) \quad \text{and} \quad \partial_t u_\varepsilon(t,x) = H * \left(\int_{\mathbb{R}} f_\varepsilon(s) \partial_{tt} \Gamma(t-s, \cdot)\, ds \right).$$

Combining the two previous facts and using Proposition 2.7 yields

$$\begin{aligned}
\mathcal{L}_1[f_\varepsilon, H] &= u_\varepsilon(\varepsilon T_f, \cdot) * \partial_t \Gamma(\varepsilon T_f, \cdot) - \partial_t u_\varepsilon(\varepsilon T_f, \cdot) * \Gamma(\varepsilon T_f, \cdot) \\
&= H * \left(\int_{\mathbb{R}} f_\varepsilon(s) \left(\partial_t \Gamma(\varepsilon T_f - s, \cdot) * \partial_t \Gamma(\varepsilon T_f, \cdot) - \partial_{tt} \Gamma(\varepsilon T_f - s, \cdot) * \Gamma(\varepsilon T_f, \cdot) \right) ds \right), \\
&= H * \left(\int_{\mathbb{R}} f_\varepsilon(s) \partial_t \Gamma(s, \cdot)\, ds \right).
\end{aligned}$$

We then infer that the operator $\mathcal{L}_1[f_\varepsilon, H]$ is a Kernel operator, in other words that

$$\mathcal{L}_1[f_\varepsilon, H] = H * K_{1, f_\varepsilon},$$

where its associated kernel K_{1,f_ε} reads

$$K_{1,f_\varepsilon}(\cdot) = \int_{\mathbb{R}} f_\varepsilon(s)\partial_t\Gamma(s,\cdot)\,ds.$$

The derivation of the second operator $\mathcal{L}_2$ is similar. Indeed, one has

$$\mathcal{L}_2[f_\varepsilon, H] = G_\varepsilon = -\partial_t w_\varepsilon(x, \varepsilon\, T_f),$$

and

$$\begin{aligned}
\mathcal{L}_2[f_\varepsilon, H] &= \partial_t u_\varepsilon(\varepsilon T_f,\cdot) * \partial_t\Gamma(\varepsilon T_f,\cdot) - u_\varepsilon(\varepsilon T_f, x) * \partial_{tt}\Gamma(\varepsilon T_f,\cdot)\\
&= H * \left(\int_{\mathbb{R}} f_\varepsilon(s)\left[\partial_{tt}\Gamma(\varepsilon T_f - s,\cdot) * \partial_t\Gamma(\varepsilon T_f,\cdot) - \partial_t\Gamma(\varepsilon T_f - s,\cdot) * \partial_{tt}\Gamma(\varepsilon T_f,\cdot)\right] ds \right),\\
&= H * \int_{\mathbb{R}} f_\varepsilon(s)\partial_{tt}\Gamma(s,\cdot)\,ds,
\end{aligned}$$

which is a kernel operator associated to the kernel

$$K_{2,f_\varepsilon}(\cdot) = \int_{\mathbb{R}} f_\varepsilon(s)\partial_{tt}\Gamma(s,\cdot)\,ds.$$

It remains to investigate the convergence properties of these operators.

Limit as $\varepsilon \to 0$. By using the finite propagation speed property of solutions of the wave equation, we claim that, for a given horizon time $T > 0$, the exists a bounded domain Ω such that the solution u_ε of (1.2) also solves

$$\begin{cases} \partial_{tt}u_\varepsilon(t,x) - \Delta u_\varepsilon(t,x) = \dfrac{df_\varepsilon}{dt}(t)H(x), & (t,x) \in \Omega \times [0,T],\\ u_\varepsilon(t,x) = 0 & (t,x) \in [-T,T] \times \partial\Omega \end{cases}$$

Notice that the function U_ε defined by $U_\varepsilon(t,x) = \int_{-\infty}^t u_\varepsilon(s,x)\,ds$ satisfies

$$\begin{cases} \partial_{tt}U_\varepsilon(t,x) - \Delta U_\varepsilon(t,x) = f_\varepsilon(t)H(x), & (t,x) \in \Omega \times [0,T],\\ U_\varepsilon(t,x) = 0 & (t,x) \in [-T,T] \times \partial\Omega \end{cases}$$

By using that $f_\varepsilon \in L^1([-T,T])$ and standard regularity results on the wave equation, we get in particular that $\|U_\varepsilon\|_{C^1([0,T],L^2(\Omega))} + \|\partial_{tt}U_\varepsilon\|_{L^1([0,T],H^{-1}(\Omega))}$, and therefore $\|u_\varepsilon\|_{C^0([0,T],L^2(\Omega))} + \|u_\varepsilon\|_{L^1([0,T],H^{-1}(\Omega))}$ is uniformly bounded with respect to ε. A standard variational analysis (see e.g. [34, Prop. 4.7]) yields in particular that $u_\varepsilon(t,\cdot)$ (respectively $\partial_t u_\varepsilon(t,\cdot)$) converges in a distributional sense to $u_0(t,\cdot)$ (respectively $\partial_t u_0(t,\cdot)$) solution of (1.1), for all $t \in [0,T]$. To conclude, let us write $H_\varepsilon(\cdot) = w_\varepsilon(\varepsilon T_f,\cdot)$ and $G_\varepsilon(\cdot) = -\partial_t w_\varepsilon(\varepsilon T_f,\cdot)$, where w_ε solves (3.1). Using the convergence result above yields that $w_\varepsilon(t,\cdot)$ also converges to $u_0(t,\cdot)$ in a distributional sense, for all $t \in [0,T]$. It follows that

$$\lim_{\varepsilon\to 0}\langle \mathcal{L}_1[f_\varepsilon, H], \varphi\rangle = \langle H, \varphi\rangle \quad \text{and} \quad \lim_{\varepsilon\to 0}\langle \mathcal{L}_2[f_\varepsilon, H], \varphi\rangle = 0.$$

for every function $\varphi \in C_c^\infty(\mathbb{R}^d)$. The desired conclusion follows.

3.2 Proof of Proposition 2.2

In this section, we provide workable and explicit expressions of the kernels K_{1,f_ε} and K_{2,f_ε}. We first start with the usual case of Gaussian functions and then we generalize to pulses in $L^2(\mathbb{R})$.

Case of Gaussian functions. Let us assume that $g(t) = \frac{1}{(4\pi)^{1/2}} \exp(-\frac{t^2}{4})$. Then its Fourier transform $\hat{g}$ writes $\hat{g}(\omega) = \exp(-\omega^2)$ and the operator $\mathcal{L}_1[g_\varepsilon, H]$ can be identified from its kernel by

$$\begin{aligned} K_{1,g_\varepsilon}(x) &= \int_{\mathbb{R}} g_\varepsilon(s)\partial_t\Gamma(s,x)\,ds = \int_{\mathbb{R}} \hat{g}(\varepsilon\omega)i\omega\Gamma_\omega(x)\,d\omega \\ &= \int_{\mathbb{R}} \sum_{p=0}^{+\infty} \frac{(-1)^p\varepsilon^{2p}\omega^{2p}}{p!} i\omega\Gamma_\omega(x)\,d\omega = \sum_{p=0}^{+\infty} \frac{(\varepsilon^2\Delta)^p}{p!}\delta_{\{x=0\}} = e^{\varepsilon^2\Delta}\left[\delta_{\{x=0\}}\right] \\ &= \frac{1}{(4\varepsilon^2\pi)^{d/2}} \exp\left(-\frac{x^2}{4\varepsilon^2}\right) = \mathcal{F}_x^{-1}\left[\exp(-\varepsilon^2|\xi|^2)\right](x) = \mathcal{F}_x^{-1}\left[\hat{g}(|\xi|\varepsilon)\right](x), \end{aligned}$$

according to Proposition 2.8.

On the other side, the kernel associate to $\mathcal{L}_2[g_\varepsilon, H]$ vanishes since g is even. Indeed, it holds

$$K_{2,g_\varepsilon}(x) = \int_{\mathbb{R}} g_\varepsilon(s)\partial_{tt}\Gamma(s,x)\,ds = -\int_{\mathbb{R}} \hat{g}(\varepsilon\omega)\omega^2\Gamma_\omega(x)\,d\omega = 0.$$

Case of a pulse f such that $\hat{f}$ is real analytic in $\mathbb{R}$. According to the decomposition of f in terms of its odd and even parts, to get the expected result, it is enough to consider the case where f is either odd or even.

Let us assume that f is even and that its Fourier transform writes

$$\hat{f}(\omega) = \sum_{p=0}^{+\infty} \alpha_{2p}\omega^{2p}.$$

Denote by $S(\mathbb{R})$ the Schwartz space (of rapidly decreasing functions).

One computes formally for every $\varphi \in S(\mathbb{R}^d)$,

$$\begin{aligned} \langle K_{1,f_\varepsilon}, \varphi\rangle &= \int_{\mathbb{R}} f_\varepsilon(s)\langle\partial_t\Gamma(s,x),\varphi(x)\rangle\,ds = \int_{\mathbb{R}} \hat{f}(\varepsilon\omega)i\omega\langle\Gamma_\omega(x),\varphi(x)\rangle\,d\omega \\ &= \int_{\mathbb{R}} \sum_{p=0}^{+\infty} \left(\alpha_{2p}\varepsilon^{2p}\omega^{2p}\right)\ i\omega\langle\Gamma_\omega(x),\varphi(x)\rangle\,d\omega = \sum_{p=0}^{+\infty} \alpha_{2p}\langle(-\varepsilon^2\Delta)^p\delta_{\{x=0\}},\varphi\rangle \\ &= \langle\mathcal{F}_x^{-1}\left[\sum_{p=0}^{+\infty}\alpha_{2p}(\varepsilon^2|\xi|^2)^p\right],\varphi\rangle = \langle\mathcal{F}_x^{-1}\left[\hat{f}(|\xi|\varepsilon)\right],\varphi\rangle \end{aligned}$$

by following the same steps as in the gaussian case, and

$$\langle K_{2,f_\varepsilon}(x),\varphi(x)\rangle = \int_{\mathbb{R}} f_\varepsilon(s)\langle\partial_{tt}\Gamma(s,x),\varphi(x)\rangle\,ds = -\int_{\mathbb{R}} \hat{f}(\varepsilon\omega)\omega^2\langle\Gamma_\omega(x),\varphi\rangle\,d\omega = 0.$$

This computation is formal. We have to justify the interchange between the sum and the integral. In this view, we claim that it is enough to work with a truncation of the series defining $\hat{f}$. For that purpose, let us introduce the kernel K^P_{1,f_ε} defined by

$$K^P_{1,f_\varepsilon} := \int_{\mathbb{R}} f^P_\varepsilon(s)\partial_t\Gamma(s,x)ds,$$

where f^P_ε is defined by

$$f^P_\varepsilon = f_\varepsilon * g_P \quad \text{with} \quad g_P(t) = \frac{P}{(4\pi)^{1/2}}\exp(-\frac{(Pt)^2}{4})$$

One has for all $\varphi \in S(\mathbb{R}^d)$,

$$\begin{aligned}
\langle K^P_{1,f_\varepsilon}, \varphi\rangle &= \langle \int_{\mathbb{R}} f^P_\varepsilon(s)\partial_t\Gamma(s,x), \varphi(x)\rangle = \langle \partial_t\Gamma(t,x), f^P_\varepsilon(t)\varphi(x)\rangle \\
&= \langle i\omega\Gamma_\omega(x), \exp(-\omega^2/P^2)\hat{f}(\varepsilon\omega)\varphi(x)\rangle = \lim_{N\to\infty}\langle i\omega\Gamma_\omega(x), \hat{f}_N(\varepsilon\omega)\exp(-\omega^2/P^2)\varphi(x)\rangle \\
&= \lim_{N\to\infty}\sum_{p=0}^{N}\langle i\omega\Gamma_\omega(x), \alpha_{2p}\varepsilon^{2p}\omega^{2p}\exp(-\omega^2/P^2)\varphi(x)\rangle \\
&= \lim_{N\to\infty}\sum_{p=0}^{N}\langle \alpha_{2p}(-\varepsilon^2\Delta)^p e^{\Delta/P}\delta_{\{x=0\}}, \varphi(x)\rangle,
\end{aligned}$$

by reproducing the computations made in the Gaussian case. Here, $\hat{f}_N$ is also defined by

$$\hat{f}_N(\omega) = \sum_{p=0}^{N}\alpha_{2p}\omega^{2p}, \quad \forall\omega\in\mathbb{R}.$$

Finally, we have

$$\langle K^P_{1,f_\varepsilon}, \varphi\rangle \quad = \quad = \lim_{N\to\infty}\langle \mathcal{F}_x^{-1}\left[\sum_{p=0}^{N}\alpha_{2p}(\varepsilon^2|\xi|^2)^p\right], e^{\Delta/P}\varphi\rangle = \langle e^{\Delta/P}\mathcal{F}_x^{-1}\left[\hat{f}(|\xi|\varepsilon)\right], \varphi\rangle.$$

Then, by letting P tend to $+\infty$, we get

$$K_{1,f_\varepsilon} = \lim_{P\to\infty} K^P_{1,f_\varepsilon} = \lim_{P\to\infty} e^{\Delta/P}\mathcal{F}_x^{-1}\left[\hat{f}(|\xi|\varepsilon)\right] = \mathcal{F}_x^{-1}\left[\hat{f}(|\xi|\varepsilon)\right],$$

the first equality being obtained by using the same reasoning as in the proof of Theorem 2.1 to compute the limit as $\varepsilon\to 0$.

Let us now assume that f is odd, determined from its Fourier transform by

$$\hat{f}(\omega) = \sum_{p=0}^{+\infty}\alpha_{2p+1}\omega^{2p+1}.$$

Then, skipping the distributional pairing for notational simplicity and using the same reasoning as in the case where f is even, one has

$$K_{1,f_\varepsilon}(x) \quad = \quad \int_{\mathbb{R}} f_\varepsilon(s)\partial_t\Gamma(s,x)\,ds = \int_{\mathbb{R}}\hat{f}(\varepsilon\omega)i\omega\Gamma_\omega(x)\,d\omega = 0$$

and

$$\begin{aligned}
K_{2,f_\varepsilon}(x) &= \int_{\mathbb{R}} f_\varepsilon(s)\partial_{tt}\Gamma(s,x)\,ds = -\int_{\mathbb{R}}\hat{f}(\varepsilon\omega)\omega^2\Gamma_\omega(x)\,d\omega \\
&= i\int_{\mathbb{R}}\sum_{p=0}^{+\infty}\left(\alpha_{2p+1}\varepsilon^{2p+1}\omega^{2p+2}\right)\ i\omega\Gamma_\omega(x)d\omega = i\frac{1}{\varepsilon}\sum_{p=0}^{+\infty}\alpha_{2p+1}(-\varepsilon^2\Delta)^{p+1}\delta_{\{x=0\}} \\
&= i\mathcal{F}_x^{-1}\left[\sum_{p=0}^{+\infty}\frac{1}{\epsilon}\alpha_{2p+1}(\varepsilon|\xi|)^{2p+2}\right] = i\mathcal{F}_x^{-1}\left[|\xi|\hat{f}(|\xi|\varepsilon)\right].
\end{aligned}$$

4 Numerics and practical implementation of the algorithm

This section is devoted to the presentation of numerical experiments highlighting the potential and the efficiency of our approach. All the numerical illustrations hereafter are restricted to the case $d = 2$. In that case, according to the Huyghens principle, we know that there does not exist a time T such that $u_\varepsilon(t,\cdot) = \partial_t u_\varepsilon(t,\cdot)$ for all $t > T$, where u_ε is the solution of (1.2). However, for each tolerance parameter

$\eta > 0$, there exists $T_\eta > 0$ such that $\sup_{t>T_\eta}(\|u_\varepsilon(t,\cdot)\|_{L^\infty(\Omega)} + \|\partial_t u_\varepsilon(t,\cdot)\|_{L^\infty(\Omega)}) \leq \eta$. By using standard continuity results on the wave operator, one can show that, provided that η be small enough (and then that T_η be large enough), the initial data $H_{\varepsilon,\eta}$ and $G_{\varepsilon,\eta}$ reconstructed by using the time reversal principal are as close as wanted to H_ε and G_ε (see [29]). This remark legitimates the use of the following algorithm, even in the case of even dimensions of space.

Time reversal algorithm for Dirac measure approximations

1. From the observation g_ε, determination of H_ε by using (for instance) the time reversal approach;
2. Deconvolution of H_ε to recover $H(\cdot)$ with the help of a deconvolution algorithm with a total variation regularization by using the explicit expression of the kernels $K_{1,f_\varepsilon}(\cdot)$ and $K_{2,f_\varepsilon}(\cdot)$ provided by Theorem 2.1.

Some practical informations on the implementation of this algorithm are provided in what follows.

4.1 Time reversal imaging and approximation

Recall that in the case where the source term is $f_0 = \delta_{\{t=0\}}$, the function u_0 satisfies

$$\begin{cases} \partial_{tt} u_0(t,x) - \Delta u_0(t,x) = 0, & (t,x) \in \mathbb{R}_+ \times \mathbb{R}^d, \\ u_0(0,x) = H(x), \quad \partial_t u_0(0,x) = 0, & x \in \mathbb{R}^d. \end{cases} \tag{4.1}$$

and the observed data g_0 are defined by

$$g_0(t,y) = u_0(t,y) \quad \text{for all } (t,y) \in [0,T] \times \partial\Omega.$$

Then the reconstruction of the source term H from g_0 can be obtained by noting that

$$H(\cdot) = w(T,\cdot),$$

where w solves the wave equation

$$\begin{cases} \partial_{tt} w(t,x) - \Delta w(t,x) = 0, & (t,x) \in [0,T] \times \Omega, \\ w(0,x) = \partial_t w(0,x) = 0, & x \in \Omega, \\ w(t,y) = g_0(T-t,y), & (t,y) \in [0,T] \times \partial\Omega. \end{cases}$$

As commented in [5], the discretization of this imaging functional requires to interpolate the data on the boundary of Ω which generates smoothing effects on the reconstructed image. From a practical point of view, it is more efficient to use an approximation version of $H(\cdot)$ reading as

$$\mathcal{I}[g_0](x) = \int_0^T v_s(T,x) ds,$$

where v_s solves the wave equation

$$\begin{cases} \partial_{tt}^2 v_s(t,x) - \Delta v_s(t,x) = \partial_t \left(\delta_{\{t=s\}} g(x, T-s) \right) \delta_{\partial\Omega}, & (t,x) \in \mathbb{R} \times \mathbb{R}^d \\ v_s(t,x) = 0, \quad \partial_t v_s(t,x) = 0, & x \in \mathbb{R}^d, t < s. \end{cases}$$

Here, $\delta_{\{t=s\}}$ denotes the time Dirac distribution at time $t = s$ and $\delta_{\partial\Omega}$ is the surface Dirac measure on the manifold $\partial\Omega$.
In particular, by using the so-called Helmholtz-Kirchhoff identity [1], it is proven in [2] that when Ω is close to a sphere in $\mathbb{R}^d$ with large radius, there holds

$$H(\cdot) \simeq \mathcal{I}[g_0](\cdot).$$

[1] Recall that, in a nutshell, this identity asserts that, for all x, z in $\mathbb{R}^d$,

$$\int_{\partial\Omega} \Gamma_\omega(x,y) \overline{\Gamma_\omega}(x,z)\, d\sigma(y) \simeq -\frac{i}{\omega} \operatorname{Im} \Gamma(x,z).$$

4.2 Description of the numerical scheme

The wave equations involved in the algorithm are solved in the box $Q = [-L/2, L/2]^2$ with periodic boundary conditions, where the size L is assumed to be sufficiently large to prevent any reflection on the boundary. Numerical integrations of each equation are then be performed exactly in the Fourier space. Let us provide some precisions on them.

Fourier space discretization. Recall that the N-Fourier approximation of a $2D$ function u in the box $Q = [-L/2, L/2]^2$ is given by

$$u^N(t,x) = \sum_{n_1,n_2=-N/2+1}^{N/2} c_{\mathbf{n}}(t) e^{2i\pi\xi_{\mathbf{n}}\cdot x},$$

where $\mathbf{n} = (n_1, n_2)$ and $\xi_{\mathbf{n}} = (n_1/L, n_2/L)$. Here the coefficient $c_{\mathbf{n}}$ represents the N^2 first discrete Fourier coefficients of u. Moreover, the inverse discrete Fourier transform of $c_{\mathbf{n}}$ allows to write that $u^N_{\mathbf{n}} = IFFT[c_{\mathbf{n}}]$ where $u^N_{\mathbf{n}} = u(x_{\mathbf{n}})$ denotes the value of the function u at the point $x_{\mathbf{n}} = (n_1 h_1, n_2 h_2)$ where $h_\alpha = L_\alpha/N$ for $\alpha \in \{1, 2\}$.

Conversely, $c_{\mathbf{n}}$ can be computed by applying the discrete Fourier transform to $u^N_{\mathbf{n}}$, namely

$$c_{\mathbf{n}} = FFT[u^N_{\mathbf{n}}].$$

Exact time integration We decide to approach the solution u of a generic wave equation

$$\partial_{tt} u(t,x) - \Delta u(t,x) = F(t,x) = \sum_{n_1,n_2=-\infty}^{+\infty} f_{\mathbf{n}}(t) e^{2i\pi\xi_{\mathbf{n}}\cdot x} \quad \text{in } \mathbb{R}\times\mathbb{R}^d$$

completed by two initial conditions, by u^N, the solution of the "truncated system"

$$\partial_{tt} u^N(t,x) - \Delta u^N(t,x) = F^N(t,x) = \sum_{n_1,n_2=-N/2+1}^{N/2} f_{\mathbf{n}}(t) e^{2i\pi\xi_{\mathbf{n}}\cdot x}$$

with two approximated initial conditions; this system also reads

$$\frac{\partial}{\partial t}\begin{pmatrix} u^N \\ u^N_t \end{pmatrix} = \begin{pmatrix} 0 & I_d \\ \Delta & 0 \end{pmatrix}\begin{pmatrix} u^N \\ u^N_t \end{pmatrix} + \begin{pmatrix} 0 \\ F^N \end{pmatrix}.$$

The last system can be integrated coefficient by coefficient, by solving the N^2 linear 2×2 systems of ordinary differential equations

$$\frac{d}{dt}\begin{pmatrix} c_{\mathbf{n}}(t) \\ c'_{\mathbf{n}}(t) \end{pmatrix} = \begin{pmatrix} 0 & 1 \\ -4\pi^2|\xi_{\mathbf{n}}|^2 & 0 \end{pmatrix}\begin{pmatrix} c_{\mathbf{n}}(t) \\ c'_{\mathbf{n}}(t) \end{pmatrix} + \begin{pmatrix} 0 \\ f_{\mathbf{n}}(t) \end{pmatrix}, \quad \text{for } \mathbf{n} = (n_1, n_2) \text{ and } n_j = -N, \dots, N \ (j = 1, 2),$$

where $c'_{\mathbf{n}}(t) = \frac{dc_{\mathbf{n}}}{dt}(t)$. Notice that this system is simple enough to be solved explicitly.

4.3 Application to photoacoustic imaging

All the numerical simulations of this section are performed with the following set of parameters:

- Ω is a two-dimensional ball of radius 1 whose boundary is discretized by 2^{10} sensors;
- the box $Q = [-L/2, L/2]^d$ has size $L = 2$ and the record time is $T = 2$;
- we use a regular step discretization with parameters $dt = T/2^{10}$ and $dx = L/2^9$.

Time reversal Imaging using ideal data g_0. On Figure 2, we use ideal data g_0 and as expected, one observes that the reconstructed source and the exact source are almost identical.

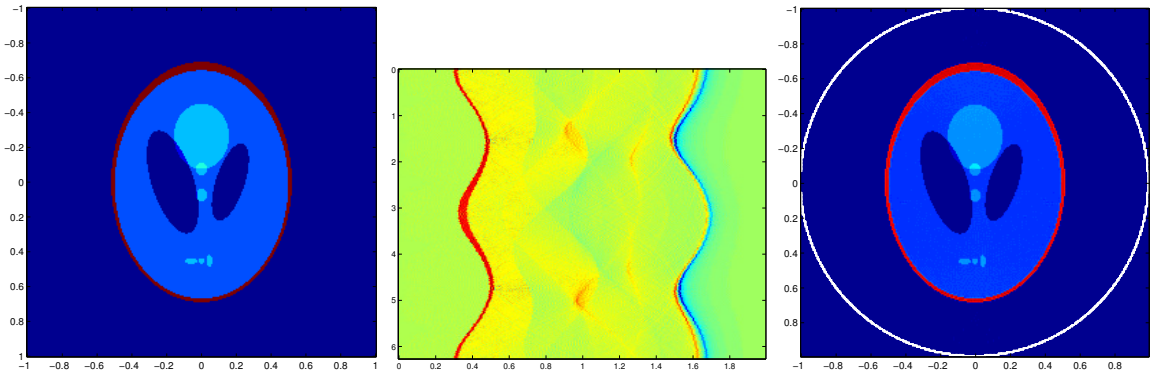

Figure 2: Source reconstruction using time reversal imaging $\mathcal{I}$; Left - initial source H, middle - given data g_0, right - $\mathcal{I}[g_0]$

Time reversal Imaging using data g_ε. We now consider three different excitation functions f_1, f_2, f_3 (see Figure 3), defined by

$$\begin{aligned} f_1(t) &= \exp(-5\pi t^2) \\ f_2(t) &= \chi_{[-1/2,1/2]}(t) \\ f_3(t) &= 3\chi_{\{-0.6,-0.2,0.2,0.6\}+[-1/12,1/12]}(t). \end{aligned}$$

On Figure 4, we observe the reconstructed source obtained by using the Imaging functional $\mathcal{I}[g_\varepsilon]$ with $\varepsilon = 0.1$.

The quality of the reconstruction does not seem not as good as in the previous case where $\varepsilon = 0$. Indeed, this is not surprising since the imaging functional $\mathcal{I}[g_\varepsilon]$ provides an efficient reconstruction of $H_\varepsilon = \mathcal{L}_1[f_\varepsilon, H]$, which can strongly differ from the source H whenever the coefficient ε is too large.

On Figure 5, the image of $H_\varepsilon = \mathcal{L}_1[f_\varepsilon, H]$ has been plotted and we observe that all the pictures correspond to the source imaging $\mathcal{I}[g_\varepsilon]$. This is a numerical illustration of the truthfulness of Theorem 2.1.

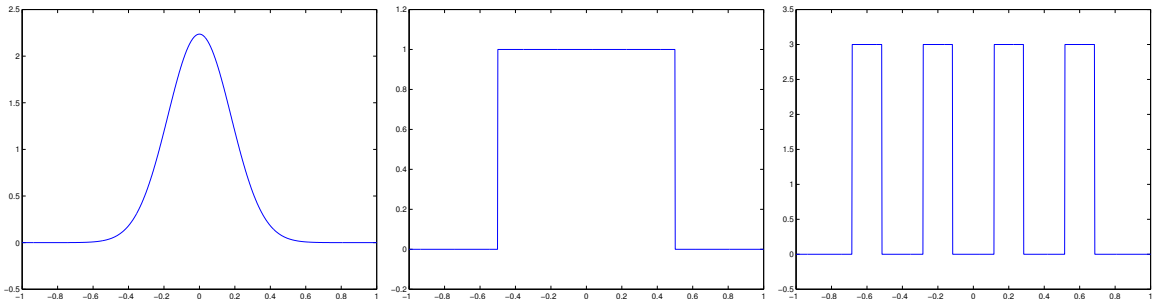

Figure 3: Plots of the three different excitation functions f_1, f_2 and f_3

Deconvolution algorithm by using a total variation regularization. In this last step of the algorithm, we reconstruct the source H from the numerical approximation $\tilde{H}_\varepsilon = \mathcal{I}[g_\varepsilon]$ by solving the

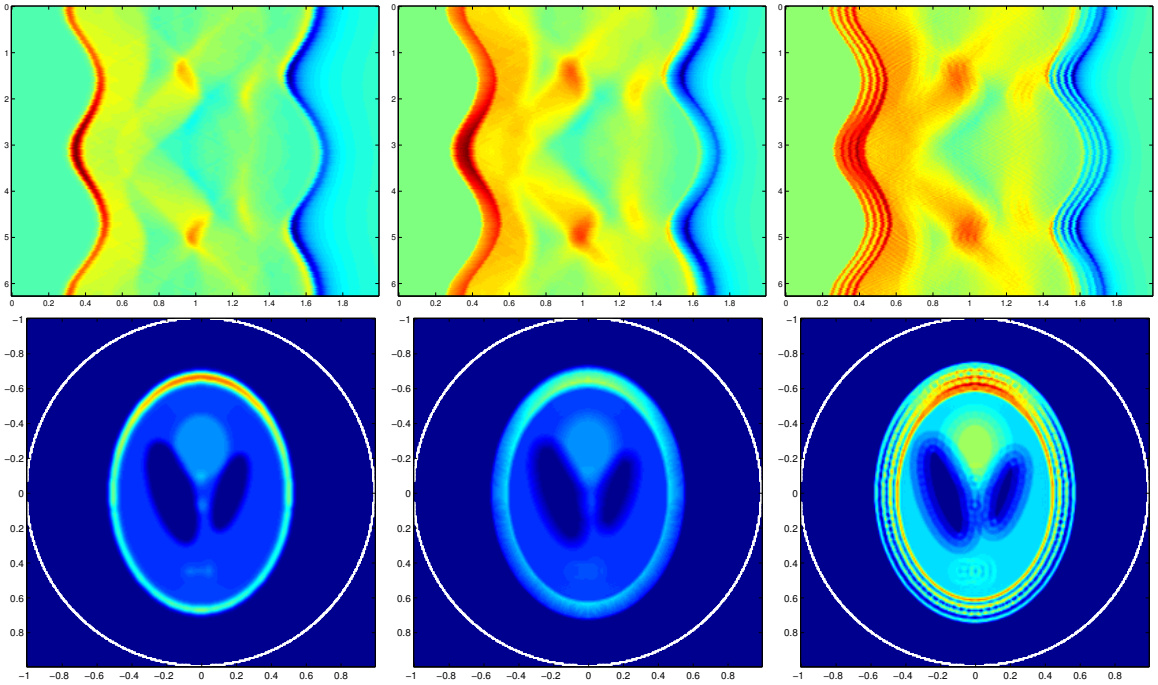

Figure 4: Time reversal imaging associated to the perturbed data g_ε ; First line : data g_ε ; second line : Imaging functional $\mathcal{I}[g_\varepsilon]$; Left to right: use of f_1, f_2 and f_3

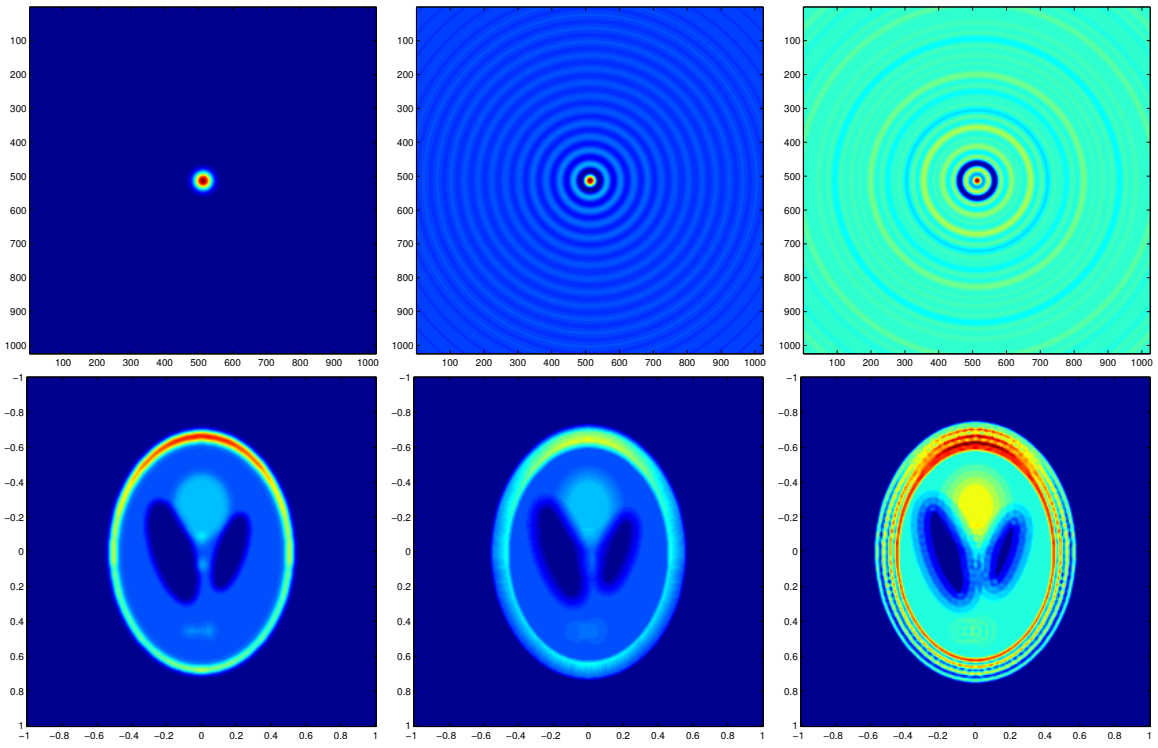

Figure 5: Kernel operator $\mathcal{L}_1[f_\varepsilon, H]$; First line : Spatial Fourier transform of the kernel K_{1,f_ε}; Second line: $\mathcal{L}_1[f_\varepsilon, H] = H * K_{1,f_\varepsilon}$; Left to right: use of f_1, f_2 and f_3

optimization problem

$$H^* = \underset{H}{\operatorname{argmin}}\{J(H)\} \quad \text{with} \quad J(H) = \frac{1}{2}\int_\Omega \left(\mathcal{I}[g_\varepsilon] - K_{1,f_\varepsilon} * H\right)^2 + \gamma \int_\Omega |\nabla H|\, dx,$$

where γ is a (positive) regularization parameter. Nevertheless, a direct computation of H^* is sometimes difficult to implement because of the non-smooth character the Total Variation (TV) term. This is why we consider an approximation of H^* with the help of an iterative *shrinkage-thresholding* algorithm [23, 21]. This algorithm can be viewed as a splitting gradient descent iterative scheme:

(0) Initialization: data g_ε, initial solution $H_0 = 0$ are known,

(1) Data link step: $H_{k+1/2} = H_k - \tau K_{1,f_\varepsilon} * [K_{1,f_\varepsilon} * H_k - \mathcal{I}[g_\varepsilon]]$,

(2) Regularization step: $H_{k+1} = T_{\gamma\tau}[H_{k+1/2}]$,

where $\tau > 0$ is a virtual descent time step and the operator T_τ is defined by

$$T_\tau[u] = \underset{v}{\operatorname{argmin}} \left\{ \frac{1}{2}\|v-u\|_{L^2(\Omega)} + \tau \|\nabla v\|_{L^1(\Omega)} \right\}.$$

The TV term is minimized implicitly by using the duality algorithm of Chambolle [20], which can be considered as an advantage of this approach. It is notable that this algorithm converges [23, 21] under a smallness assumption on the parameter τ, namely $\tau \|\mathcal{F}[K_{1,f_\varepsilon}]\|_\infty^2 \leq 1$. A possible variant consists in considering the algorithm by Beck and Teboulle [14] to accelerate the convergence rate. On Figure 6, the reconstructed source H^* obtained for the three different functions f_1, f_2 and f_3 are plotted.

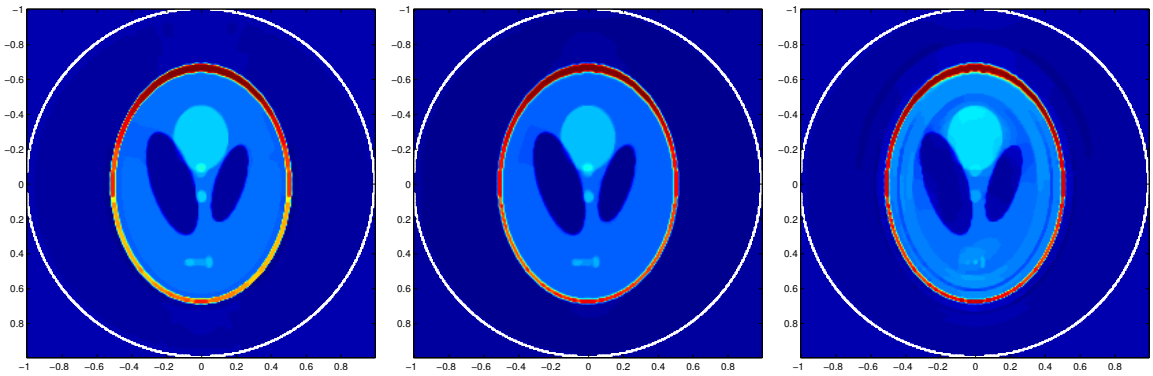

Figure 6: Correction of the source reconstruction using deconvolution algorithm with total variation regularization; Left to right : using f_1, f_2 and f_3

Influence of ε :
We finally present some numerical experiments using the pulse f_3 and associated to different values of ε. On Figure 7 and for $\varepsilon = 0.075$, $\varepsilon = 0.1$ and $\varepsilon = 0.15$, we plot respectively the data g_ε, the reconstruction of the source using the classical Time Reversal Imaging and the reconstruction of the source after applying the deconvolution algorithm. In particular, we can observe an influence of ϵ on the localization of the waves and as expected, the reconstruction of the source is even better than ε is small.

5 Generalization to elasticity wave operators

The motivation of this section is to emphasize that our approach can be extended without special effort to many kinds of wave equation involving homogeneous operators in space. In particular, having in mind

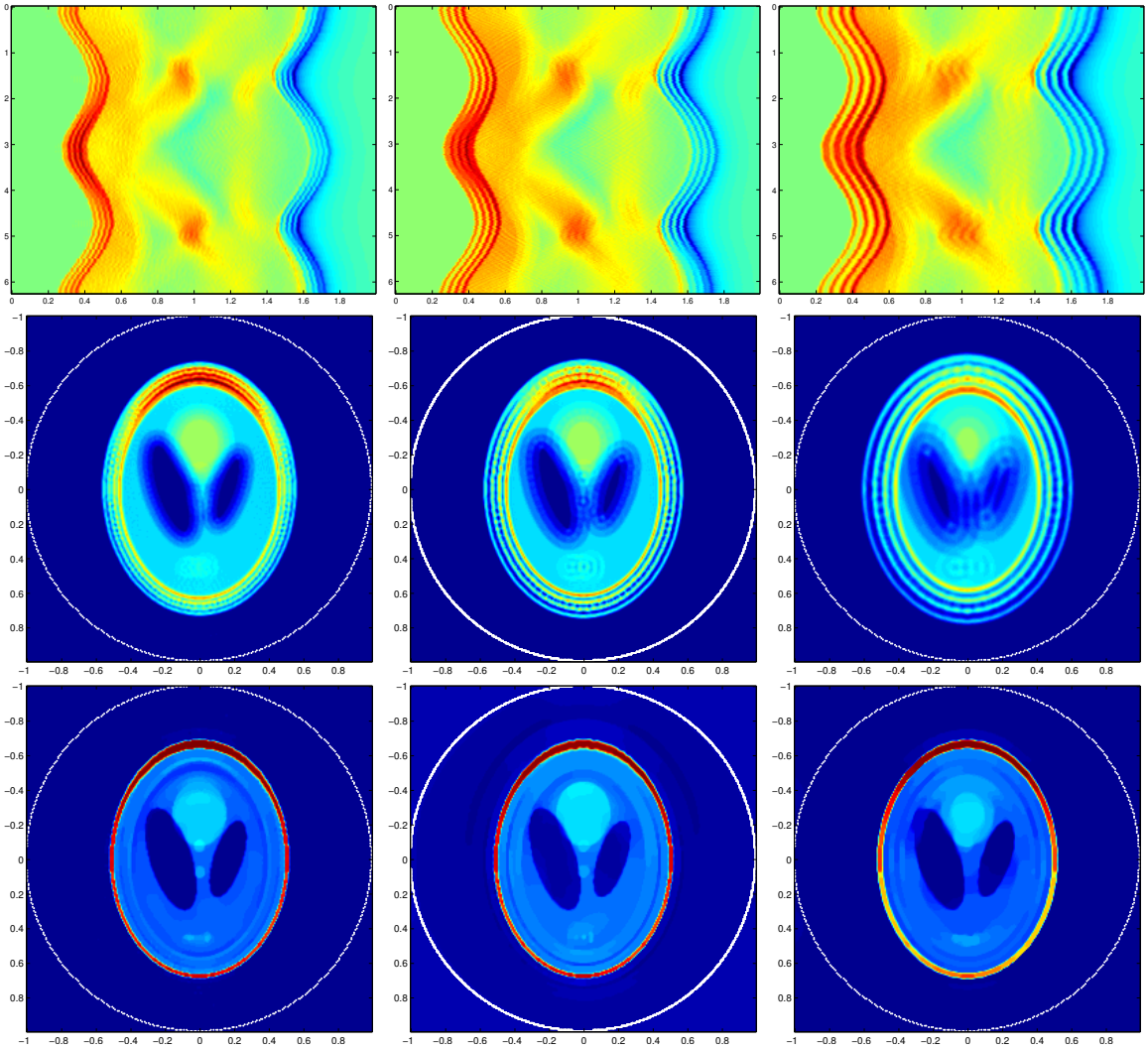

Figure 7: Influence of the parameter ε on the reconstruction of the source in the case of the pulse f_3 ; First line : the data g_ε ; Second line : reconstruction using Time reversal imaging associated to g_ε ; Last line : correction of the source reconstruction using deconvolution algorithm with total variation regularization ; Left to right : with respectively $\varepsilon = 0.075$, $\varepsilon = 0.1$ and $\varepsilon = 0.15$.

some recent advances on hybrid methods in biomedical imaging exploiting elastic properties of the soft tissue [9, 10, 8, 16, 27, 40], we focus on the linear elastic wave equation. For the sake of clarity and since all proofs follow exactly the same lines as those of Section 3, we will only provide the main steps allowing to extend our results to the framework of elastic waves.

Let us now consider the homogeneous isotropic elastic wave equation in a d-dimensional open medium

$$\begin{cases} \partial_{tt}\mathbf{u}_\varepsilon(t,x) - \mathcal{L}_{\lambda,\mu}\mathbf{u}_\varepsilon(t,x) = f_\varepsilon'(t)\mathbf{H}(x), & (t,x) \in \mathbb{R}\times\mathbb{R}^d, \\ \mathbf{u}_\varepsilon(x,t) = \partial_t\mathbf{u}_\varepsilon(t,x) = \mathbf{0}, & x \in \mathbb{R}^d,\ t < -\varepsilon T_f, \end{cases}$$

where

$$\mathcal{L}_{\lambda,\mu}\mathbf{u} = \mu\Delta\mathbf{u} + (\lambda+\mu)\nabla(\nabla\cdot\mathbf{u}).$$

Here (λ,μ) denote the Lamé coefficients of the medium. The inverse problem we consider here is to reconstruct the source $\mathbf{H}$ from the data set

$$\mathbf{g}_\varepsilon(t,y) = \mathbf{u}_\varepsilon(t,y), t \in [0,T], y \in \partial\Omega.$$

Case of ideal data: $\varepsilon = 0$. In the ideal case with $\varepsilon = 0$, we are led to consider the function $\mathbf{u}_0$ solution of

$$\begin{cases} \partial_{tt}\mathbf{u}_0(t,x) - \mathcal{L}_{\lambda,\mu}\mathbf{u}_0(t,x) = \delta'_{t=0}\mathbf{H}(x), & (t,x) \in \mathbb{R}\times\mathbb{R}^d, \\ \mathbf{u}_0(t,x) = \partial_t\mathbf{u}_0(t,x) = \mathbf{0}, & x \in \mathbb{R}^d,\ t<0, \end{cases}$$

and

$$\mathbf{g}_0(t,y) = \mathbf{u}_0(t,y), t \in [0,T], y \in \partial\Omega.$$

It has been recently addressed in [19, 6, 4]. More precisely, it is proven that the natural imaging functional $\mathcal{I}$ defined by

$$\mathcal{I}[\mathbf{g}_0](x) = \int_0^T \mathbf{v}_s(T,x)ds, \quad x \in \Omega,$$

where the vector field $\mathbf{v}_s$ is defined as the solution of

$$\begin{cases} \partial_{tt}\mathbf{v}_s(t,x) - \mathcal{L}_{\lambda,\mu}\mathbf{v}_s(t,x) = \dfrac{d\delta_{t=s}}{dt}\mathbf{g}_0(T-s,y)\delta_{y=\partial\Omega}, & (t,x) \in \mathbb{R}\times\mathbb{R}^d, \\ \mathbf{v}_s(t,x) = \partial_t\mathbf{v}_s(t,x) = \mathbf{0}, & x \in \mathbb{R}^d,\ t<s. \end{cases} \tag{5.1}$$

does not lead to a sufficiently good reconstruction of the source $\mathbf{H}$. A more efficient reconstruction [6] can then be obtained by considering the following modified version

$$\widetilde{\mathcal{I}}[\mathbf{g}_0] = c_s\nabla\times\psi_{\mathcal{I}} + c_p\nabla\phi_{\mathcal{I}}. \tag{5.2}$$

Here $c_p = \sqrt{\lambda+2\mu}$ and $c_s = \sqrt{\mu}$ denote respectively the pressure and the shear wave speeds and $\psi_{\mathcal{I}}$ and $\phi_{\mathcal{I}}$ represent the compressional and the shear components of $\mathcal{I}$ respectively which are defined from the Helmholtz decomposition of $\mathcal{I}$:

$$\mathcal{I} = \nabla\times\psi_{\mathcal{I}} + \nabla\phi_{\mathcal{I}}. \tag{5.3}$$

In the sequel, we define respectively the Helmholtz decomposition operator $\mathcal{H}^p$ and $\mathcal{H}^s$ by

$$\mathcal{H}^p[\mathcal{I}] = \nabla\phi_{\mathcal{I}} \quad \text{and} \quad \mathcal{H}^s[\mathcal{I}] = \nabla\times\psi_{\mathcal{I}}.$$

Green function and equivalent Cauchy problem. Let us also introduce the outgoing Green's tensor $\mathbb{G}_{\omega,0}$ associated to the elastic wave equation

$$(\mathcal{L}_{\lambda,\mu} + \omega^2)\mathbb{G}_\omega(x) = -\delta_{\mathbf{x}=\mathbf{0}}\mathbb{I}, \qquad x \in \mathbb{R}^d.$$

and $\mathbb{G}$, the temporal version of the previous Green tensor, defined as the range by the inverse Fourier transform of $\mathbb{G}_\omega$, in other words

$$\mathbb{G}(t,\cdot) = \mathcal{F}_t^{-1}[\mathbb{G}_\omega(\cdot)](t).$$

Using the same arguments as in the acoustic case, we can show the equivalent of Proposition 2.7.

Proposition 5.1. *For all $t \in [0,s]$, there holds*

$$\begin{cases} \partial_t\mathbb{G}(t,\cdot) & = \partial_t\mathbb{G}(s-t,\cdot) * \partial_t\mathbb{G}(s,\cdot) - \partial_{tt}\mathbb{G}(t,\cdot) * \mathbb{G}(s-t,\cdot) \\ \mathbb{G}(t,\cdot) & = \mathbb{G}(t,\cdot) * \partial_t\mathbb{G}(s-t,\cdot) - \partial_t\mathbb{G}(t,\cdot) * \mathbb{G}(s-t,\cdot) \end{cases} \quad \text{in } \mathcal{D}'(\mathbb{R}^d).$$

In particular, considering $t=0$, we obtain the identity:

$$\forall s>0, \qquad \delta_{\mathbf{x}=\mathbf{0}}\mathbb{I} = \partial_t\mathbb{G}(s,\cdot) * \partial_t\mathbb{G}(s,\cdot) - \partial_{tt}\mathbb{G}(s,\cdot) * \mathbb{G}(s,\cdot) \tag{5.4}$$

Moreover, the proof of the following theorem follows exactly the same line as the one of Theorem 2.1.

Theorem 5.2. *Let $T_f > 0$, $\varepsilon > 0$, Ω be a connected bounded open set of $\mathbb{R}^d$ and K be a compact set such that $K \subset \Omega$. Then, for all $\mathbf{H}$ such that $\mathrm{supp}(\mathbf{H}^s) \subset K$ and $\mathrm{supp}(\mathbf{H}^p) \subset K$ where $\mathbf{H}^s$ and $\mathbf{H}^p$ are defined from the Helmoltz decomposition of $\mathbf{H}$:*

$$\mathbf{H}^s = \mathcal{H}^s[\mathbf{H}], \quad \text{and} \quad \mathbf{H}^p = \mathcal{H}^p[\mathbf{H}], \tag{5.5}$$

and for $\varepsilon > 0$ small enough, there exists a Cauchy problem

$$\begin{cases} \partial_{tt}\mathbf{v}_\varepsilon(t,x) - \mathcal{L}_{\lambda,\mu}\mathbf{v}_\varepsilon(t,x) = \mathbf{0}, & (t,x) \in \mathbb{R}_+ \times \mathbb{R}^d, \\ \mathbf{v}_\varepsilon(0,x) = \mathbf{H}_\varepsilon(x) \text{ and } \quad \partial_t \mathbf{v}_\varepsilon(0,x) = \mathbf{G}_\varepsilon(x) & x \in \mathbb{R}^d \end{cases}$$

equivalent to (5.1) in the sense that

$$\mathbf{u}_\varepsilon(t,y) = \mathbf{v}_\varepsilon(t,y), \quad \forall (t,y) \in [0,T] \times \partial\Omega.$$

Moreover, $\mathbf{H}_\varepsilon$ and $\mathbf{G}_\varepsilon$ are given by

$$\mathbf{H}_\varepsilon = \mathcal{L}_1[f_\varepsilon, \mathbf{H}] = \mathbf{K}_{1,f_\varepsilon} * \mathbf{H}, \quad \text{and} \quad \mathbf{G}_\varepsilon = \mathcal{L}_2[f_\varepsilon, \mathbf{H}] = \mathbf{K}_{2,f_\varepsilon} * \mathbf{H},$$

where

$$\mathbf{K}_{1,f_\varepsilon}(\cdot) = \int_{\mathbb{R}} f_\varepsilon(s)\partial_t \mathbb{G}(s,\cdot)\, ds \quad \text{and} \quad \mathbf{K}_{2,f_\varepsilon}(\cdot) = \int_{\mathbb{R}} f_\varepsilon(s)\partial_{tt}\mathbb{G}(s,\cdot) ds,$$

Explicit expression of the associated kernels. The reconstruction of $\mathbf{H}$ from the knowledge of $\mathbf{H}_\varepsilon$ can then be performed by using the Helmholtz decomposition of $\mathbf{H}_\varepsilon$ as well as two deconvolution procedures. In particular, the explicit expression of each kernel is derived from the proposition below.

Proposition 5.3. *Let $f \in L^2(\mathbb{R})$ be defined from its Fourier transform $\hat{f}$ given in $\mathbb{R}^d$ by*

$$\hat{f}(\omega) = \sum_{n=0}^{+\infty} \alpha_n \omega^n,$$

and let us introduce the four following scalar kernel

$$K^\alpha_{1,f_\varepsilon}(x) = \mathcal{F}_x^{-1}\left[\hat{f}_e(|\xi| c_\alpha \varepsilon)\right] \text{ and } K^\alpha_{2,f_\varepsilon}(x) = i\mathcal{F}_x^{-1}\left[|\xi|\hat{f}_o(|\xi| c_\alpha \varepsilon)\right], \quad \alpha \in \{s,p\},$$

where f_e and f_o denote the even and odd parts of f respectively. Then we have

$$\mathbf{K}_{1,f_\varepsilon} * \mathbf{H} = K^p_{1,f_\varepsilon} * \mathbf{H}^p + K^s_{1,f_\varepsilon} * \mathbf{H}^s$$

and

$$\mathbf{K}_{2,f_\varepsilon} * \mathbf{H} = K^p_{2,f_\varepsilon} * \mathbf{H}^p + K^s_{2,f_\varepsilon} * \mathbf{H}^s,$$

where $\mathbf{H}^p$ and $\mathbf{H}^s$ are given by (5.5).

The proof of this proposition is essentially based on the Helmholtz decomposition of $\mathbb{G}_\omega$, namely $\mathbb{G}_\omega = \mathbb{G}^s_\omega + \mathbb{G}^p_\omega$, and on the following remark

$$\mathcal{L}_{\lambda,\mu}[\mathbb{G}^p_\omega] = c_p^2 \Delta \mathbb{G}^p_\omega \quad \text{and} \quad \mathcal{L}_{\lambda,\mu}[\mathbb{G}^s_\omega] = c_s^2 \Delta \mathbb{G}^s_\omega$$

and that, for $\alpha \in \{s,p\}$,

$$\int_{\mathbb{R}} (-1)^p \omega^{2p} i\omega \mathbb{G}^\alpha_\omega(\cdot)\, d\omega = c_\alpha^{2p} \Delta^p(\mathcal{H}^\alpha\left[\delta_{\{x=0\}}\mathbb{I}\right]) \quad \text{and} \quad \int_{\mathbb{R}} (-1)^p \omega^{2p} \mathbb{G}^\alpha_\omega(\cdot)\, d\omega = 0.$$

Finally, the source of $\mathbf{H}$ can be reconstructed by finding separately it compressional and shear components which can be done for instance by using a TV-deconvolution approach :

$$\mathbf{H}^{\alpha,*} = \underset{\mathbf{H}}{\operatorname{argmin}} \{J_\alpha(\mathbf{H})\} \quad \text{with} \quad J_\alpha(\mathbf{H}) = \frac{1}{2}\int_\Omega \left(\mathcal{H}\left[\widetilde{\mathcal{I}}[\mathbf{g}_\varepsilon]\right]^\alpha - K^\alpha_{1,f_\varepsilon} * \mathbf{H}\right)^2 + \gamma \int_\Omega |\nabla \mathbf{H}|\, dx.$$

6 Comments and conclusion

In this article, we have proposed a systematic method allowing to reconstruct the spatial component of a source term whose temporal component cannot be approximated by a Dirac mass. The proposed algorithm rests upon the use of an imaging technique based on a time reversal approach, and a correction of the reconstructed source with the help of a TV regularization-deconvolution algorithm.

Some first numerical experiments allowed to validate the method in the acoustic framework and we claim that our method is robust enough to be extended to many kinds of wave-like operators involving homogeneous space operators, such as linear elasticity wave ones.

Finally, the approach developed in this article highlights a connexion between a regularization in time and in space, where the respective kernels sizes are correlated to the wave velocity.

We are actually investigating the issue of exploiting/generalizing this approach to tackle inverse problems in non-homogenous media where the main unknown is the wave velocity.

Acknowlegments

This work have been supported by the ANR (AVENTURES - ANR-12-BLAN-BS01-0001-01).
Y. Privat was partially supported by the Project "Analysis and simulation of optimal shapes - application to lifesciences" of the Paris City Hall.

References

[1] H. Akhouayri, M. Bergounioux, A. Da Silva, A. Litman, and M. Mindrinos. Quantitative thermoacoustic tomography with microwaves sources. *To appear in Journal of Inverse and Ill-posed Problems*.

[2] H. Ammari. *An Introduction to Mathematics of Emerging Biomedical Imaging*. Mathematics & Applications, Vol. 62, Springer-Verlag, Berlin, 2008.

[3] H. Ammari, E. Bossy, V. Jugnon, and H. Kang. Mathematical modeling in photoacoustic imaging of small absorbers. *SIAM Rev.*, 52(4):677–695, 2010.

[4] H. Ammari, E. Bretin, J. Garnier, H. Kang, H. Lee, and A. Wahab. *Mathematical Methods in Elasticity Imaging*. Princeton University Press, Princeton, NJ, USA, 2015.

[5] H. Ammari, E. Bretin, J. Garnier, and A. Wahab. Time reversal in attenuating acoustic media. In *Mathematical and statistical methods for imaging*, volume 548 of *Contemp. Math.*, pages 151–163. Amer. Math. Soc., Providence, RI, 2011.

[6] H. Ammari, E. Bretin, J. Garnier, and A. Wahab. Time-reversal algorithms in viscoelastic media. *European J. Appl. Math.*, 24(4):565–600, 2013.

[7] H. Ammari, E. Bretin, V. Jugnon, and A. Wahab. Photoacoustic imaging for attenuating acoustic media. In *Mathematical modeling in biomedical imaging. II*, volume 2035 of *Lecture Notes in Math.*, pages 57–84. Springer, Heidelberg, 2012.

[8] H. Ammari, L. G. Bustos, H. Kang, and H. Lee. Transient elasticity imaging and time reversal. *Proceedings of the Royal Society of Edinburgh: Section A Mathematics*, 141(6):1121–1140, 2011.

[9] H. Ammari, P. Garapon, L. G. Bustos, and H. Kang. Transient anomaly imaging by the acoustic radiation force. *Journal of Differential Equations*, 249(7):1579 – 1595, 2010.

[10] H. Ammari, P. Garapon, H. Kang, and H. Lee. A method of biological tissues elasticity reconstruction using magnetic resonance elastography measurements. *Quarterly of Applied Mathematics*, 66(1):139–175, 2008.

[11] G. Bal and K. Ren. Multi-source quantitative photoacoustic tomography in a diffusive regime. *Inverse Problems*, 27(7):075003, 20, 2011.

[12] G. Bal and G. Uhlmann. Inverse diffusion theory of photoacoustics. *Inverse Problems*, 26(8):085010, 20, 2010.

[13] C. Bardos and M. Fink. Mathematical foundations of the time reversal mirror. *Asymptot. Anal.*, 29(2):157–182, 2002.

[14] A. Beck and M. Teboulle. A fast iterative shrinkage-thresholding algorithm for linear inverse problems. *SIAM J. Imaging Sci.*, 2(1):183–202, 2009.

[15] Z. Belhachmi, T. Glatz, and O. Scherzer. A direct method for photoacoustic tomography with inhomogeneous sound speed. *Inverse Problems*, 32(4):045005, 25, 2016.

[16] J. Bercoff, M. Tanter, M. Mulle, and M. Fink. The role of viscosity in the impulse diffraction field of elastic waves induced by the acoustic radiation force. *IEEE Trans. Ultrasonics, Ferro., Freq. Control*, 51(6):1523–1536, 2004.

[17] M. Bergounioux, X. Bonnefond, T. Haberkorn, and Y. Privat. An optimal control problem in photoacoustic tomography. *Math. Models Methods Appl. Sci.*, 24(12):2525–2548, 2014.

[18] R. I. Brevis, J. H. Ortega, and D. Pardo. A source time reversal method for seismicity induced by mining. *Inverse Probl. Imaging*, 11(1):25–45, 2017.

[19] S. Catheline, N. Benech, J. Brum, and C. Negreira. Time reversal of elastic waves in soft solids. *Phys. Rev. Lett.*, 100:064301, Feb 2008.

[20] A. Chambolle. An algorithm for total variation minimization and applications. *J. Math. Imaging Vision*, 20(1-2):89–97, 2004. Special issue on mathematics and image analysis.

[21] P. L. Combettes and V. R. Wajs. Signal recovery by proximal forward-backward splitting. *Multiscale Model. Simul.*, 4(4):1168–1200, 2005.

[22] B. T. Cox, J. G. Laufer, and P. C. Beard. The challenges for quantitative photoacoustic imaging, 2009.

[23] I. Daubechies, M. Defrise, and C. De Mol. An iterative thresholding algorithm for linear inverse problems with a sparsity constraint. *Comm. Pure Appl. Math.*, 57(11):1413–1457, 2004.

[24] L. C. Evans. *Partial differential equations*, volume 19 of *Graduate Studies in Mathematics*. American Mathematical Society, Providence, RI, second edition, 2010.

[25] D. Finch, M. Haltmeier, and Rakesh. Inversion of spherical means and the wave equation in even dimensions. *SIAM J. Appl. Math.*, 68(2):392–412, 2007.

[26] M. Fink. Time-reversal acoustics. In *Inverse problems, multi-scale analysis and effective medium theory*, volume 408 of *Contemp. Math.*, pages 151–179. Amer. Math. Soc., Providence, RI, 2006.

[27] J. Greenleaf, M. Fatemi, and M. Insana. Selected methods for imaging elastic properties of biological tissues. *Annual Review of Biomedical Engineering*, 5:57–78, 2003.

[28] M. Haltmeier, T. Schuster, and O. Scherzer. Filtered backprojection for thermoacoustic computed tomography in spherical geometry. *Math. Methods Appl. Sci.*, 28(16):1919–1937, 2005.

[29] Y. Hristova. Time reversal in thermoacoustic tomography—an error estimate. *Inverse Problems*, 25(5):055008, 14, 2009.

[30] Y. Hristova, P. Kuchment, and L. Nguyen. Reconstruction and time reversal in thermoacoustic tomography in acoustically homogeneous and inhomogeneous media. *Inverse Problems*, 24(5):055006, 25, 2008.

[31] R. Kowar. Integral equation models for thermoacoustic imaging of acoustic dissipative tissue. *Inverse Problems*, 26(9):095005, 18, 2010.

[32] R. Kowar, O. Scherzer, and X. Bonnefond. Causality analysis of frequency-dependent wave attenuation. *Math. Methods Appl. Sci.*, 34(1):108–124, 2011.

[33] P. Kuchment and O. Scherzer. *Tomography, Photoacoustic, and Thermoacoustic*, pages 1488–1496. Springer Berlin Heidelberg, Berlin, Heidelberg, 2015.

[34] K. Kunisch, P. Trautmann, and B. Vexler. Optimal control of the undamped linear wave equation with measure valued controls. *SIAM J. Control Optim.*, 54(3):1212–1244, 2016.

[35] L. A. Kunyansky. Explicit inversion formulae for the spherical mean Radon transform. *Inverse Problems*, 23(1):373–383, 2007.

[36] T. Liu, J. Wang, G. Petrov, V. Yakovlev, and H. Zhang. Photoacoustic generation by multiple picosecond pulse excitation. *Med Phys.*, 37(3):1518–1521, 2010.

[37] S. Mandelbrojt. Quasi-analycité des séries de Fourier. *Ann. Scuola Norm. Sup. Pisa Cl. Sci. (2)*, 4(3):225–229, 1935.

[38] L. V. Nguyen. A family of inversion formulas in thermoacoustic tomography. *Inverse Probl. Imaging*, 3(4):649–675, 2009.

[39] G. Paltauf, R. Nuster, M. Haltmeier, and P. Burgholzer. Experimental evaluation of reconstruction algorithms for limited view photoacoustic tomography with line detectors. *Inverse Problems*, 23(6):S81–S94, 2007.

[40] A. P. Sarvazyan, O. V. Rudenko, S. D. Swanson, J. Fowlkes, and S. Y. Emelianov. Shear wave elasticity imaging: a new ultrasonic technology of medical diagnostics. *Ultrasound in Medicine & Biology*, 24(9):1419 – 1435, 1998.

[41] O. Scherzer, M. Grasmair, H. Grossauer, M. Haltmeier, and F. Lenzen. *Variational methods in imaging*, volume 167 of *Applied Mathematical Sciences*. Springer, New York, 2009.

[42] L. Schwartz. Transformation de Laplace des distributions. *Comm. Sém. Math. Univ. Lund [Medd. Lunds Univ. Mat. Sem.]*, 1952(Tome Supplémentaire):196–206, 1952.

[43] M. Tanter and M. Fink. *Time Reversing Waves For Biomedical Applications*, pages 73–97. Springer Berlin Heidelberg, Berlin, Heidelberg, 2009.

[44] Q. Z. Tianheng Wang, Patrick D. Kumavor. Application of laser pulse stretching scheme for efficiently delivering laser energy in photoacoustic imaging. *Journal of Biomedical Optics*, 17:17 – 17 – 9, 2012.

[45] M. Xu and L. V. Wang. Photoacoustic imaging in biomedicine. *Review of scientific instruments*, 77(4):041101–041101, 2006.